NASA Technical Memorandum 83311

Traction Behavior of Two Traction Lubricants

S. H. Loewenthal and D. A. Rohn
Lewis Research Center
Cleveland, Ohio

Prepared for the
Annual Meeting of the American
Society of Lubrication Engineers
Houston, Texas, April 24–29, 1983

NASA

Traction Behavior of Two Traction Lubricants

by S. H. Loewenthal and D. A. Rohn

National Aeronautics and Space Administration
Lewis Research Center
Cleveland, Ohio 44135

ABSTRACT

In the analysis of rolling-sliding concentrated contacts, such as gears, bearings and traction drives, the traction characteristics of the lubricant are of prime importance. The elastic shear modulus and limiting shear stress properties of the lubricant dictate the traction/slip characteristics and power loss associated with an EHD contact undergoing slip and/or spin. These properties can be deduced directly from the initial slope m and maximum traction coefficient μ of an experimental traction curve. In this investigation, correlation equations are presented to predict m and μ for two modern traction fluids based on the regression analysis of 334 separate traction disk machine experiments. The effects of contact pressure, temperature, surface velocity, ellipticity ratio are examined. Problems in deducing lubricant shear moduli from disk machine tests are discussed.

E-1507

INTRODUCTION

The traction characteristics of a lubricant are of great importance to the performance of many machine elements, such as bearings, gears, and traction drives. In the case of traction drives, the maximum traction coefficient furnished by the lubricant determines the useful traction hence torque that can be transmitted without slip. The effective traction coefficient occurring in the contact also dictates the amount of slip occurring in ball bearings, the skew in roller bearings, and the creep rate across a traction-drive contact. The product of the traction force and slip rate is a direct measure of the load-dependent power loss of a rolling-element contact.

In this regard, there have been a number of theoretical investigations to predict the performance of a traction elastohydrodynamic (EHD) contact, based on the rheological characteristics of lubricant (refs. 1 to 6). Contact pressure, temperature, shear rates, and lubricant composition all play important roles on whether the lubricant film exhibits viscous behavior or acts as an elastic material. It is now generally accepted (refs. 6 to 9) that in most rolling-element contacts, the lubricant behaves elastically at small rates of strain, that is, at low sliding speeds. At higher sliding speeds, the lubricant film exhibits highly nonlinear viscous behavior and tends to shear or "yield" like a plastic-solid. Thus the lubricant's behavior in a traction contact can be modeled with reasonable accuracy as an elastic-plastic material having some characteristic shear modulus G and some limiting or critical yield stress τ_c (ref. 7). These two lubricant parameters, which vary with pressure, temperature, velocity, and contact geometry, must be determined under the appropriate operating conditions before traction contact performance calculations can be performed (ref. 10).

In a typical traction contact, severe transient operating conditions are imposed on the lubricant. The lubricant is swept into the contact, exposed to contact pressures, which are 10 000 times atmospheric or greater,

and returned to ambient conditions, all in a few milliseconds. Because of the difficulty of simulating the highly transient nature of an actual traction contact, fluid property data that has been deduced from an experimental traction curve (ref. 6) has traditionally given more satisfactory results in traction calculations than primary measurements from oscillatory shear viscosimeters or similar laboratory equipment. In particular, elastic shear moduli data determined from primary measurements (ref. 11) are much larger than those deduced from EHD traction measurements. However, recent limiting shear stress measurements under isothermal compression reported in ref. 12 has shown reasonable agreement with those from EHD traction tests (ref. 6).

In references 6, 10, and 13, Johnson and Tevaarwerk present a comprehensive traction-contact analysis, applicable to traction drives, which incorporates the lubricant's shear modulus and limiting shear stress in the form of several dimensionless parameters. These parameters can be written in terms of the maximum traction coefficient μ and initial slope m from an experimental traction curve, using the transformation methods described in refs. 6 and 10. Traction data of this type has been relatively scarce, particularly for modern traction fluids, over sufficiently broad enough operating conditions for design purposes (refs. 14 to 17) [illegible]ef. 18, experimental traction data were obtained for two modern t[illegible]n fluids, Santotrac 50 and TDF-88, over a rang[illegible] of speeds, pressures, t[illegible]ratures, contact ellipticity ratios, spin, and sideslip values that might be encountered in traction drives. A multi-variable regression analysis of this data was performed by the authors (ref. 19). In this investigation the correlation equations resulting from this analysis will be used to study the effects of the primary variables on μ and m for these two fluids. The variation of the fluids fundamental properties, shear modulus G and limiting shear stress τ_c will be investigated as well.

NOMENCLATURE

a	contact ellipse semi-width in y-direction (transverse to direction of rolling), m
A_{11}, A_{22}	Kalker coefficients in x and y direction, respectively.
b	contact ellipse semi-width in x-direction (rolling), m
C	lubricant factor defined in eq. (3)
$C_1,\ldots,C_8$	slope and traction coefficient correlation coefficients
E	modulus of elasticity, GPa
$\overline{G}_f$	mean elastic shear modulus of the film, GPa
$\overline{G}^*$	mean apparent elastic shear modulus of the contact system (film + disks), GPa
h	elastohydrodynamic central film thickness, m
k	contact ellipse ratio, a/b
m	initial slope of the traction curve (film + disk)
m_d	dry initial slope of the traction curve (disk only)
m^*/m	slope correction factor, eq. (6)
P	maximum contact pressure, GPa
$\overline{P}$	mean contact pressure, GPa

R_x equivalent relative radii of curvature in x-direction (rolling), m

$$= \left(\frac{1}{r_{AX}} + \frac{1}{r_{BX}}\right)^{-1}$$

r_{AX}, r_{BX} principal rolling radii of bodies A and B, m
T temperature, °C
U average rolling surface velocity in x-direction, m/s
ΔU longitudinal (x-direction) slip velocity, m/s
μ maximum traction coefficient
μ_x longitudinal traction coefficient
ν Poisson's ratio
$\bar{\tau}_c$ limiting "yield" shear stress of film, GPa
ω_s angular spin velocity, sec^{-1}

PERFORMANCE PREDICTIONS

In the 1960's and early 1970's, many papers were presented on the prediction of traction in EHD contacts (refs. 3, 20 and 21). About this time, Poon (ref. 4) and Lingard (ref. 5) developed grid methods for shear stress integration to predict the available traction forces of a contact experiencing spin. Poon's method utilized the basic traction data from a twin-disk machine together with contact kinematics to predict the available traction. Lingard used a theoretical approach in which the EHD film exhibited a Newtonian viscous behavior at low shear rates until a critical limiting shear stress was reached. At this point the film yielded plastically with increasing shear rate. The most recent and perhaps most comprehensive traction-contact model is that proposed by Johnson and Tevaarwerk (refs. 6, 10, and 13). Their model covers the full range of viscous, elastic, and plastic behavior of the EHD film. This type of behavior depends on the Deborah number, a relative measure of elastic-to-inelastic response, and the strain rate. At low pressures and speeds (low Deborah number), the film exhibits linear viscous behavior at low strain rates. It becomes increasingly more nonlinear with increasing strain rate. At higher pressures and speeds, more typical of traction-drive contacts, the response is linear and elastic at low rates of strain. At sufficiently high strain rates, the shear stress reaches some limiting value and the film shears like a plastic solid as in the case of some of the earlier traction analytical models (refs. 2, 4 and 5).

In refs. 10 and 13, Tevaarwerk presents graphical solutions developed from the Johnson and Tevaarwerk elastic-plastic traction model. Several dimensionless parameters were identified that best generalized the results of their analysis. These parameters were written in terms of the mean shear modulus of the contact $\bar{G}^*$, that is, the lubricant film/disk combination, and mean limiting shear stress properties of the lubricant film $\bar{\tau}_c$. Since shear modulus $\bar{G}^*$ and limiting shear stress $\bar{\tau}_c$ data are generally difficult to

obtain, as an alternative, these dimensionless groupings can be written in terms of the initial slope m and maximum traction coefficient μ from an experimental traction curve from the following relations (refs. 10 and 11):

$$\bar{G}^* = m\left(\frac{h}{b}\right)\bar{P} \qquad (1)$$

$$\bar{\tau}_c = \mu\,\bar{P} \qquad (2)$$

where $\bar{P}$ is the average contact pressure, h is the central EHD film thickness, b is the semi-ellipse diameter in the rolling direction. The parameters m and μ are to be obtained from a zero-spin/zero-sideslip curve at the same contact pressure, temperature, rolling speed, and for the same ellipticity ratio, area, and disk material as the contact to be analyzed. However, it is possible to use data obtained from tests where the ellipticity ratio and contact area are different if certain corrections for the compliance of the disk material are made to the slope as given in refs. 10, 13 and 19.

With the Johnson and Tevaarwerk analysis, knowing just m and μ from a simple traction test leads to the prediction of the isothermal traction-creep curve under any combination of sideslip and spin. Also, the traction force transverse to the rolling direction and contact power losses can be readily determined. As an example, under the specialized case where there is no spin or side-slip present, a simple relationship exists between traction and slip of the form:

$$\frac{\mu_x}{\mu} = \frac{1}{\pi}\left(2\tan^{-1} S + \frac{2S}{1+S^2}\right) \qquad (3)$$

where

$$S = \frac{2}{3}\,C\,\frac{(\Delta U)}{U}\Big/\sqrt{k}$$

$$C = \frac{\bar{G}^*}{\bar{\tau}_c}\left(\frac{b}{h}\right)\sqrt{k} \quad \text{or} \quad \frac{3\pi}{8}\left(\frac{m}{\mu}\right)\sqrt{k}$$

TRACTION FLUID DATA

To be able to apply a traction performance analysis, such as the Johnson and Tevaarwerk model, to the evaluation of a traction contact, μ and m must be determined at the appropriate operating condition. Recently, experimental traction data of this type were obtained in ref. 18 for Santotrac 50

and TDF-88 traction fluids over the range of operating conditions that might be encountered in a traction drive. The properties of these lubricants appear in table I. Overall, 187 and 147 separate traction tests were conducted on the Santotrac 50 and TDF-88 test fluids, respectively. Maximum contact pressures ranged from 1.0 to 1.9 GPa; rolling speeds from 10 to 80 m/sec; oil inlet temperatures from 17 to 73° C; contact ellipse ratios from 1 to 5; and spin angles from 0 to 30°.

A twin-disk traction tester which is described in ref. 18 was used to generate the traction data. Basically, the tester consists of a transversely crowned upper disk which is driven by a cylindrical lower disk powered by a variable-speed electric motor. The upper disk is dead-weight loaded against the lower disk. The upper disk is supported in a cradle that is free to pivot around a vertical axis to generate a sideslip velocity. The resulting traction forces transmitted through the cradle are measured with a load cell. The cradle can also tilt the upper disk as to generate angular spin velocity. The transverse radius of curvature of the upper disk can be varied to alter the contact ellipticity ratio.

REGRESSION ANALYSIS

In ref. 19, a multi-variable regression analysis was applied to the data generated in ref. 18. A total of 187 traction coefficients and 73 slope data points were analyzed for the Santotrac 50 fluid and 147 traction coefficient and 101 slope data points for the TDF-88 fluid. After evaluating several forms of the regression equation, the following expression was found to best represent the data with the fewest terms:

$$\mu = C_1 + C_2P + C_3P^2 + C_4U + C_5U^2 + C_6T + C_7k + C_8\frac{\omega_s\sqrt{ab}}{U} \qquad (4)$$

$$m = C_1 + C_2P + C_3\ln(P) + C_4U + C_5U^2 + C_6T + C_7k + C_8\frac{\omega_s\sqrt{ab}}{U} \qquad (5)$$

The coefficients of this correlation equation for each of the test fluids are given in table II. The correlation's regression coefficient R, a measure of the fit of the regression equation, was greater than 0.88 for the traction coefficient and greater than 0.80 for slope for either fluid. (An R-value of 0 indicates no correlation while an R-value of 1.0 indicates a perfect correlation.) A representative comparison of predicted and measured traction coefficient data for the Santotrac 50 test fluid appears in Fig. 1. With a modest extrapolation of the test conditions, the likely useable range of Eqs. (4) and (5) is for maximum pressures of 1.0 to 2.5 GPa; surface velocities from 1.0 to 100 m/sec; inlet temperatures from 30 to 100° C; ellipticity ratios from 0.5 to 8; and dimensionless spin $\omega_s\sqrt{ab}/U$ from 0 to 0.04.

To illustrate the application of the regression equations (4) and (5), traction versus slip curves for Santotrac 50 were calculated at a representative operating condition using Eq. (3). A comparison of the predicted (lines) and measured data (symbols) for this case appears in Fig. 2. It is clear that the maximum traction coefficient and slope diminishes with increased velocity. The data shows that traction reaches a maximum at a slip

value of about 0.005 under the given operating conditions and then slowly decreases with larger slip as thermal effects become more prominent. The simple isothermal expression of Eq. (3), of course, is not useful in the large slip region without thermal corrections such as those given in refs. 22 and 23.

Slope Correction

The slope of an experimental traction curve is a measure of the tangential stiffness or apparent shear modulus $\bar{G}^*$ of the lubricant film and metal surface combination. When the film is thin and stiff, as it is at low speeds and high pressures, the tangential deformation or compliance of the disk material is not negligible in comparison. Since the slope produced by the disks in dry contact, i.e., without a lubricant film, is independent of the disk size while that produced by the film and disk system is not, then a change in disk size will affect the measured slope of the film/disk system even if all of the remaining operating variables are kept the same. Thus to use slope data generated under identical operating conditions, but with disk of different size, an adjustment must be made. This adjustment can be made under the assumption that the elastic shear modulus of the film alone $\bar{G}_f$ will not be affected by changes in disk size under identical operating conditions. Based upon this assumption and the simplification that the contact compliance is the simple summation of the film compliance and disk compliance, an approximate slope correction factor was developed in ref. 19 for steel rollers as follows:

$$\frac{m^*}{m} = \left\{ \left(\frac{R_x}{R_x^*} \right)^{0.67} + 7.66 \times 10^{-3} m \, Pe^{-0.21/k} \left[1 - \frac{A_{11}}{A_{22}} \left(\frac{R_x}{R_x^*} \right)^{0.67} \right] \right\}^{-1} \qquad (6)$$

where m^*/m is the slope correction factor, R_x/R_x^* is the ratio of the test disk equivalent radius to the equivalent radius of the disks to be analyzed, P is the maximum contact pressure in GPa, k is the contact ellipse ratio and A_{11}/A_{22} is the ratio of Kalker's coefficients (ref. 24) in the x and y direction. This ratio can be satisfactorily approximated by the following expression:

$$\frac{A_{11}}{A_{22}} = 1.43 - 0.383/k + 0.0995/k^2 \qquad (7)$$

The slope correlation equation (5) is based on data generated with disks having an equivalent radius R_x of 22.57 mm in the case of Santotrac 50 and an R_x of 12.50 mm in the case of TDF-88. If the disks to be analyzed (denoted by the astericked parameters) have an R_x^* different than that above, then Eq. (6) may be solved to determine the appropriate correction factor m^*/m. The m^*/m factor then can be applied to the m value calculated from the correlation Eq. (5) to obtain the corrected slope m^*

for the case in question. Typically, for a contact having a $k = 5$, lubricated with TDF-88 at $P = 1.5$ GPa, the m^*/m factor will vary from about 0.8 for disks of 10 mm in equivalent radius to about 1.9 for disks of 100 mm in radius.

RESULTS AND DISCUSSION

Effect of Operating Conditions

As mentioned before, knowledge of μ and m and the effects that operating conditions have on them is of great importance in the optimization of a traction mechanism. The correlations Eqs. (4) and (5) can be conveniently used to study the effects that speed, pressure, spin, and lubricant type have on these traction performance factors.

Effect of speed and pressure. - As shown in Figs. 3 and 4, μ and m tend to benefit to a certain point from a reduction in surface velocity and from an increase in contact pressure. Increases in pressure tend to increase the film's resistance to shear, that is, its viscosity and/or "yield" shear strength. This is illustrated in Fig. 5 where the mean limiting shear stress $\bar{\tau}_c$ (computed from Eqs. (2) and (4)) is plotted against pressure, velocity and temperature for Santotrac 50. However, as indicated by Fig. 3, the maximum traction coefficient, which is the ratio of $\bar{\tau}_c$ to $\bar{P}$, reaches some limiting value at some pressure (near 2 GPa), beyond which there is little or no gain. This has been observed by others (refs. 16 and 22).

The correlated slope data in Fig. 4 also shows an increase with pressure, to a certain point, as the film's stiffness, that is shear modulus, increases. However, at pressures in the vicinity of 1.5 GPa, the compliance of the disk material (steel) begins to become more pronounced causing a gradual reduction in the apparent slope of the film/disk contact.

Increases in surface velocity are detrimental to μ and m. The loss in traction is due to the increase in lubricant film thickness which varies approximately with surface velocity to 0.7 power. As shown in the thermal analysis of refs. 22 and 23, thick films hinder the heat transfer from the center plane of the film to the cooler disk surface, thereby raising the center plane film temperature. As with most materials, increases in film temperature tend to reduce the "shear strength" of the film and thus reduce its effective traction coefficient. Degradation of $\bar{\tau}_c$ with increased velocity and inlet temperature, to a lesser extent, is apparent from Fig. 5. The traction coefficient and slope correlated data in Figs. 3 and 4 tend to reach some minimum value with increasing speed. This is consistent with the observation that film thickness tends to reach some maximum limiting value with increasing speed due to thermal and starvation effects.

Effect of spin. - Spin, the result of a mismatch in roller radii at contact points on either side of the point of pure rolling, has a detrimental effect on traction performance as illustrated in Fig. 6. It occurs in contacts having conical or contoured rolling-elements, such as an angular contact bearing, where the intersection of the tangent to the point of contact and the axes of rotation are noncoincident. Spin creates a circular slip

velocity pattern which disrupts useful traction, that is the component of traction oriented in the rolling direction. It also contributes to spin heating which also reduces the shear strength of the film by way of higher film temperatures. Spin not only limits the maximum traction which can be imposed across the contact without gross slip, as evidenced by Fig. 6, but also leads to higher slip values, $\Delta U/U$, at any given value of traction. The higher slip values coupled with the dissipative torque or twisting moment due to spin leads to higher contact power losses. At low values of spin, that is for $\omega_s\sqrt{ab}/U$ less than approximately $1 \Big/ \left[\frac{3\pi}{8}\left(\frac{m}{\mu}\right)\sqrt{k}\right]$, most of the contact is being strained elastically (energy is recoverable) so the power loss penalty is small (refs. 10 and 13). At higher levels of spin, losses increase almost directly with spin as the lubricant film yields plastically.

Fig. 7 shows that not all lubricants have the same sensitivity to spin. It is apparent that the TDF-88 fluid shows a smaller reduction in μ with nondimensional spin, $\omega_s\sqrt{ab}/U$, than does the Santotrac 50 fluid. At zero-spin, the Santotrac 50 fluid shows a small advantage in μ at the operating condition chosen but across the range of operating conditions analyzed, this advantage is not particularly significant. The μ of the Santotrac 50 fluid also shows a somewhat greater sensitivity to P but for either fluid there is little incentive in operating above about 2.0 GPa.

Rheological Properties

It is now well-established (ref. 25) that the linear region of the traction curve is governed by the visco-elastic properties of the lubricant. At the pressures, temperatures and speeds associated with a typical, traction carrying, EHD contact (lubricant viscosities exceeding about 10^5 Pa-s), the lubricant is thought to be in the "glassy" state exhibiting solid-like shear behavior. At small strain rates, the behavior is elastic in nature characterized by the combined elastic shear modulus of the film and disk material $\bar{G}^*$. At higher strain rates approaching the peak traction point, non-linear viscous flow deformation occurs which can be modeled as a material "yielding" plastically at some critical or limiting shear stress $\bar{\tau}_c$. This limiting shear stress can be readily deduced from the maximum traction coefficient value of an experimental traction curve from the relation shown in Eq. (2). The typical effects of pressure, temperature and velocity on $\bar{\tau}_c$ from the correlated traction coefficient data of Santotrac 50 appear in Fig. 5. Limiting shear stress values deduced in this manner tend to agree with recent high pressure, isothermal compression, viscometer measurements reported in ref. 12. For example, limiting shear stress values reported in ref. 12 of 0.068 and 0.112 GPa at mean pressures of 0.6 and 1.0 GPa respectively for Santotrac 50 at 25° C compare favorably with $\bar{\tau}_c$ of 0.061 and 0.115 GPa found from Eq. (2) and the correlated data Eq. (4) (at an estimated 1 m/s). Similar agreement was reported in ref. 12 with $\bar{\tau}_c$ data for other oils determined by traction disk measurements performed in ref. 6.

Elastic modulus of film. - Since the initial gradient of traction-slip curve is the result of a linear elastic response, it should be possible, in principle, to extract the elastic shear modulus of the film $\bar{G}_f$ from the measured slope of the film and disk material combination. As rightfully pointed out in ref. 25, it is not easy to do this reliably due to the considerable elastic deformation contributed by the disk material particularly at the higher contact pressures. This point will be illustrated by the discussion which follows.

In ref. 11, a method to determine elastic shear moduli of lubricants from disk machine tests is described. The method is based on a numerical integration of the tangential traction distribution throughout the elastic region of the contact, recognizing that the film will only strain elastically in the center of the contact where the pressure is sufficiently high. The elastic region was defined by some critical pressure P_c at which the transition from viscous to elastic response occurs. Based on this critical pressure P_c and the ratio of the measured slope to the slope produced by the disks in dry rolling contact, m/m', graphical solutions were presented in ref. 25 for a shear modulus correction factor $\bar{G}_f/\bar{G}^*$. This correction factor is to be applied to the apparent, mean modulus of the film and disk system $\bar{G}^*$ to find the mean modulus of the film alone, $\bar{G}_f$. The system modulus $\bar{G}^*$ is directly related to the measured slope m as shown in Eq. (1).

Eq. (1) was used together with the modulus correction factor from Ref. 25 to calculate the shear modulus of the film $\bar{G}_f$ for both the Santotrac 50 and TDF-88 traction data. Fig. 8 shows a plot of $\bar{G}_f$ against the maximum contact pressure for the 73 Santotrac 50 slope data points covering the complete range of test conditions. It is apparent there is considerable variability in the results. This is also the case for the TDF-88 data which is not shown. However, there is general magnitude agreement with Santotrac 50 modulus data and modulus data for Santotrac 40 from ref. 11, represented by the solid line appearing in Fig. 8. Santotrac 40 is essentially a lower viscosity version of the Santotrac 50 fluid without the additive package. The Santotrac 40 modulus data in ref. 11 came from traction disk tests at 30° C with disk sets made of both steel and tungsten carbide. As discussed in ref. 11, shear moduli data from traction disk experiments at higher pressures are significantly smaller than those obtained from oscillatory shear experiments, perhaps due to transient effects.

There are two significant problems in deducing the film shear modulus from the slope of a traction curve. The first is getting sufficient definition of the initial portion of the traction curve in the region of extremely small slip values ($\Delta U/U$ less than about .0005) so that the interpolated slope truly represents the linear elastic region. Just a 0.5 degree error in the slope line, say 88.5 degrees instead of 88 degrees (using a square grid) means a 33 percent error in slope, that is a slope of 38.2 versus 28.6 in this example. A second and equally formidable problem is that at the higher pressures, greater than about 1.0 GPa at lower speeds and higher temperatures (thin EHD film), the compliance or tangential deformation of the disk mate-

rial accounts for much of total compliance of the contact. Under these conditions, it is difficult to accurately ascertain the compliance or conversely stiffness (a measure of shear modulus) of the thin, stiff EHD film when its compliance represents a small fraction of the total. The problem is analogous to accurately determining the stiffness of a stiff spring in series with a soft one from the total deflection of the two spring system. For example, at a maximum pressure of 1 GPa, temperature of 67° C, velocity of 20 m/s and aspect ratio of 1.0, the apparent shear modulus of the shear modulus of the film and disk system $\bar{G}$ was found to be only 0.135 GPa while the modulus of the film alone is estimated to be 1.09 GPa using the correction methods of ref. 25. Thus the effective film stiffness is about 8 times that of the system.

In the above example, the correction factor is based on the steel disk material used in the traction tests described herein. Had tungsten carbide disks been used, as used in the tests of ref. 25, the correction for disk compliance would have been greatly reduced since the effective elastic modulus for tungsten carbide is more than 3 times larger than that for steel ($E/(1 - \nu^2)$ = 767 GPa versus 230 GPa for steel). More consistent shear modulus measurements would be expected with the tungsten carbide disks since their compliance would have a much smaller effect on the system slope, particularly at the higher operating pressures.

The exaggerated effect that the disk compliance factor and small variations in slope have on the deduced film shear modulus are illustrated in Figs. 9 and 10. Fig. 9 shows a comparison of the film shear modulus predicted from the Santotrac 50 slope correlation Eq. (5), at the conditions noted, with the film modulus given in ref. 25 for Santotrac 40. The deviations occuring between 1.5 and 2.5 GPa are quite large. However, comparing the predicted slope from Eq. (5) (solid line) and the slope required to produce the linear modulus results of ref. 25 (dashed line) as shown in Fig. 10, the discrepancy in slope is surprisingly small, well within the accuracy of the slope measurements. It is evident that even small variations in measured slope at the higher pressures can lead to drastic changes in the modulus correction factor and hence the deduced shear modulus of the film. The results presented here corroborate the warning given in ref. 25 that "the determination of shear modulus from disk machine traction tests is a very imprecise process."

SUMMARY AND CONCLUSIONS

The results of a regression analysis performed on 334 experimental traction curves for two traction fluids are presented. Regression equations relating the maximum traction coefficient μ and initial slope m to contact pressure, velocity, temperature, contact ellipse ratio and spin are given. Slope corrections are given for the analysis of contacts having a different size than those used in generating the slope data. The parameters μ and m are useful, in conjunction with a traction performance model, for prediction of the traction/slip characteristics and power loss associated with an EHD contact undergoing various combinations of slip, sideslip and spin.

Based on the correlated data, the Santotrac 50 and TDF-88 fluids generally exhibited comparable traction behavior. The TDF-88 fluid did display a somewhat reduced sensitivity to the adverse effects of spin. Increases in

pressure caused a corresponding increase in μ, reaching some upper limit at maximum contact pressures in the vicinity of 2.0 GPa. The slope was also observed to increase with pressure, reaching a maximum at about 1.5 GPa and diminishing thereafter as the compliance of the steel disks became increasingly more pronounced. Increases in temperature, surface velocity, ellipticity ratio and spin generally caused a reduction in μ and m. However, the reductions due to velocity became increasingly less at higher speed.

The deduced limiting or "yield" shear stress of the test fluids exhibited a near linear increase with pressure.

Considerable variability was encountered in extracting the effective shear modulus of either fluid from the slope test data. This variability is attributed to the lubricant film's rather small contribution to the total compliance of the contact, particularly at the higher contact pressures. Consequently, small variations in the measured slope can cause drastic changes in the calculated modulus of the film. The use of high modulus material for the disks, such as tungsten carbide in place of steel, would help reduce the masking effect of disk compliance.

REFERENCES

1. Poritsky, H., Hewlett, C. W., Jr., and Coleman, R. E, Jr., "Sliding Friction of Ball Bearings of the Pivot Type," J. Appl. Mech., 14, (4), A-261 to A-268 (1947).
2. Wernitz, W., "Friction at Hertzian Contact with Combined Roll and Twist," Rolling Contact Phenomena, ed. by J. B. Bidwell, Elsevier Publishing Co. (1962), pp. 132-156.
3. Cheng, H. S., and Sternlicht, B., "A Numerical Solution for the Pressure, Temperature, and Film Thickness Between Two Infinitely Long Lubricated Rolling and Sliding Cylinders Under Heavy Loads," J. Basic Eng., ASME Trans., 87, (3), 695-707 (1965).
4. Poon, S. Y., "Some Calculations to Assess the Effect of Spin on the Tractive Capacity of Rolling Contact Drives," Proc. Inst. Mech. Eng. (London), 185, (76/71), 1015-1022 (1970).
5. Lingard, S., "Tractions at the Spinning Point Contacts of a Variable Ratio Friction Drive," Tribol. Int., 7, (5), 228-234 (1974).
6. Johnson, K. L., and Tevaarwerk, J. L., "Shear Behavior of Elastohydrodynamic Oil Films," Proc. R. Soc. (London), Ser. A., 356, (1685), 215-236 (1975).
7. Clark, O. H., Woods, W. W., and White, J. R., "Lubrication at Extreme Pressure with Mineral Oil Films," J. of Appl. Phys., 22, (4), 474-483 (1951).
8. Johnson, K. L., and Cameron, R., "Shear Behavior of Elastohydrodynamic Oil Films at High Rolling Contact Pressures," Proc. Inst. Mech. Eng. (London), 182, (14), 307-319 (1967).
9. Bair, S., and Winer, W. O., "Shear Strength Measurements of Lubricants at High Pressures," J. of Lub. Technol., ASME Trans., 101, (3), 251-257 (1979).
10. Tevaarwerk, J. L., "Traction Drive Performance Prediction for the Johnson and Tevaarwerk Traction Model," National Aeronautics and Space Administration, NASA TP-1530 (1979).

11. Johnson, K. L., Nayak, L., and Moore, A. J., "Determination of Elastic Shear Modulus of Lubricants from Disc Machine Tests," Elastohydrodynamics and Related Topics, ed. by D. Dowson, Mech. Eng. Publ. Ltd., (1979) pp. 204-213.
12. Bair, S., and Winer, W. O., "Some Observations in High Pressure Rheology of Lubricants," J. of Lub. Technol., ASME Trans., 104, (3), 357-364 (1982).
13. Tevaarwerk, J. L., and Johnson, K. L., "The Influence of Fluid Rheology on the Performance of Traction Drives," J. of Lub. Technol., ASME Trans., 101, (3), 266-274 (1979).
14. Walowit, J. A., and Smith, R. L., "Traction Characteristics of a MIL-L-7808 Oil," ASME Paper No. 76-Lubs-19 (1976).
15. Hewko, L. O., Rounds, F. G., Jr., and Scott, R. L., "Tractive Capacity and Efficiency of Rolling Contacts," Rolling Contact Phenomena, ed. by J. B. Bidwell, Elsevier Publishing Co. (Amsterdam) (1962), pp. 157-185.
16. Gaggermeier, Helmut, "Investigations of Tractive Force Transmission in Variable Traction Drives in the Area of Elastohydrodynamic Lubrication," Ph.D. Dissertation, Technical University of Munich (1977).
17. Gupta, P. K., Flamand, L., Berthe, D., and Godet, M., "On the Traction Behavior of Several Lubricants," J. of Lub. Technol., ASME Trans., 103, (1), 55-64 (1981).
18. Tevaarwerk, J. L., "Traction Contact Performance Evaluation at High Speeds," National Aeronautics and Space Administration, NASA CR-165226 (1981).
19. Loewenthal, S. H.; and Rohn, D. A.: Regression Analysis of Traction Characteristics of Two Traction Fluids. NASA TP-2099, 1983.
20. Dowson, D., and Whitaker, B. A., "A Numerical Procedure for the Solution of Elastohydrodynamic Problem of Rolling and Sliding Contacts Lubricated by a Newtonian Fluid," Proc. Inst. of Mech. Eng. (London), 108, (3B), 57-71 (1966).
21. Kannel, J. W., and Walowit, J. A., "Simplified Analysis for Tractions Between Rolling-Sliding Elastohydrodynamic Contacts," J. Lubr. Technol., Trans. ASME, 93, (1) 39-46 (1971).
22. Johnson, K. L., and Greenwood, J. A., "Thermal Analysis of an Eyring Fluid in Elastohydrodynamic Traction," Wear, 61, 353-374 (1980).
23. Tevaarwerk, J. L., "Thermal Influence on the Traction Behavior of an Elastic/Plastic Model," Presented at the Leeds/Lyon Conference on Tribology, Leeds, England, (Aug. 1980).
24. Kalker, J. J., "On the Rolling Contact of Two Elastic Bodies in the Presence of Dry Friction," Ph.D. Dissertation, Rept. No. WTHD-52, Technische Hogeschool, Delft (1973).
25. Johnson, K. L., "Introductory Review of Lubricant Rheology and Traction Elastohydrodynamics and Related Topics," Elastohydrodynamics and Related Topics, ed. by D. Dowson, Mech. Engr. Publ. Ltd. (1979), pp. 155-161.

TABLE I. - TRACTION LUBRICANT PROPERTIES

Property	Lubricant description	
	Santotrac 50	TDF-88
Kinomatic viscosity, cm^2/sec (cS) at		
311 K (100° F)	0.34 (34)	0.42 (42)
372 K (210° F)	0.056 (5.6)	0.054 (5.4)
Flash point, K (°F)	435 (325)	408 (275)
Fire point, K (°F)	447 (345)	428 (310)
Autoignition temperature, K (°F)	600 (620)	--- ---
Pour point, K (°F)	236 (-35)	236 (-35)
Specific heat at 311 K (100° F), J/kg.K (Btu/lb °F)	2130 (0.51)	1895 (.45)
Thermal conductivity at 311 K (100° F), $J/m^8.sec.K$ ($Btu/hr.ft^8.°F$)	0.10 (0.06)	0.11 (0.066)
Specific gravity at 311 K (100° F)	0.889	0.888

TABLE II. - COEFFICIENTS FOR REGRESSION EQUATIONS (4) AND (5)

Coef	Initial Slope, m		Max Traction Coeff., μ	
			Santotrac 50	TDF-88
C_1	101.4	51.3	0.0726	0.0733
C_2	-45.48	-6.53	0.0477	0.0443
C_3	69.44	17.20	-0.0102	-0.0116
C_4	-0.288	-0.646	-6.92×10^{-4}	-7.36×10^{-4}
C_5	1.30×10^{-3}	4.99×10^{-3}	2.74×10^{-6}	2.38×10^{-6}
C_6	6.63×10^{-2}	0.236	-2.13×10^{-4}	-9.08×10^{-5}
C_7	-2.99	-1.24	-3.4×10^{-4}	-1.88×10^{-3}
C_8	0	0	-1.22	-0.443

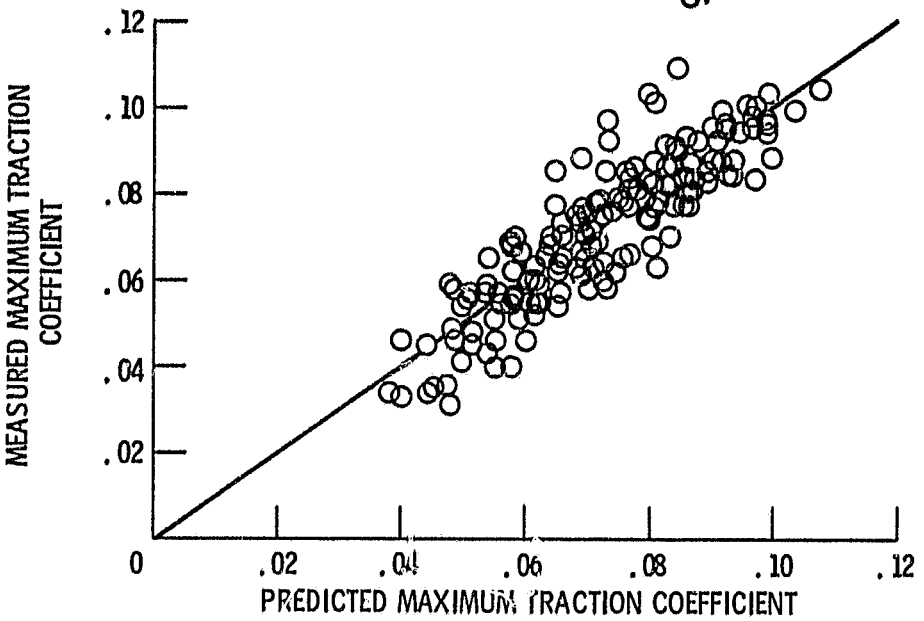

Figure 1. - Comparison of predicted and measured maximum traction coefficient Santotrac 50 data from (18).

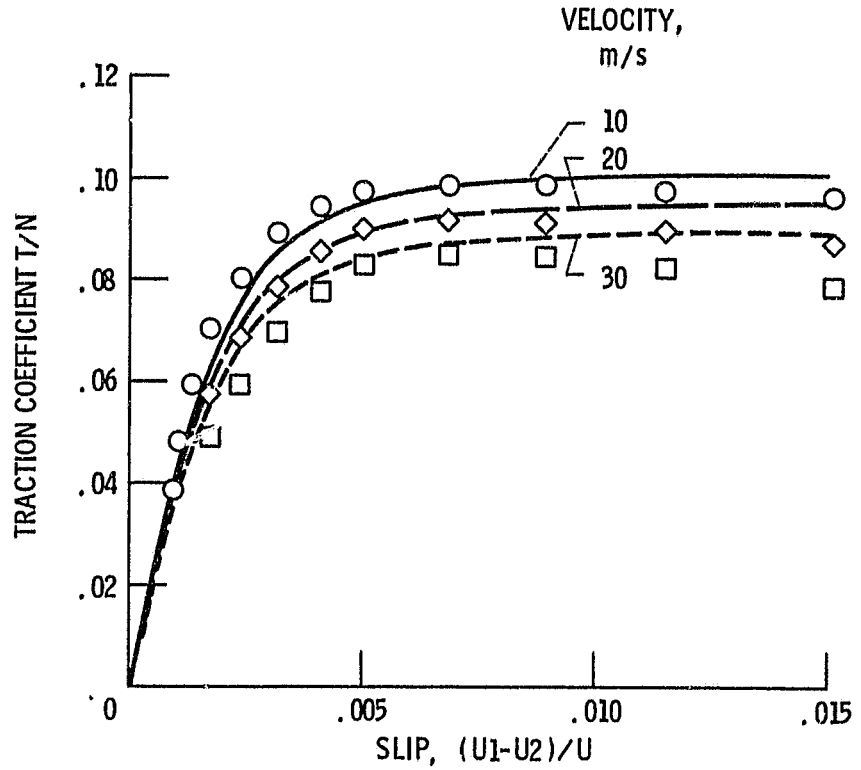

Figure 2. - Comparison of predicted and measured traction coefficient versus slip curves Santotrac 50. Pressure, 1.23 GPa; temperature, 30° C; ellipticity ratio, 5; spin, 0.

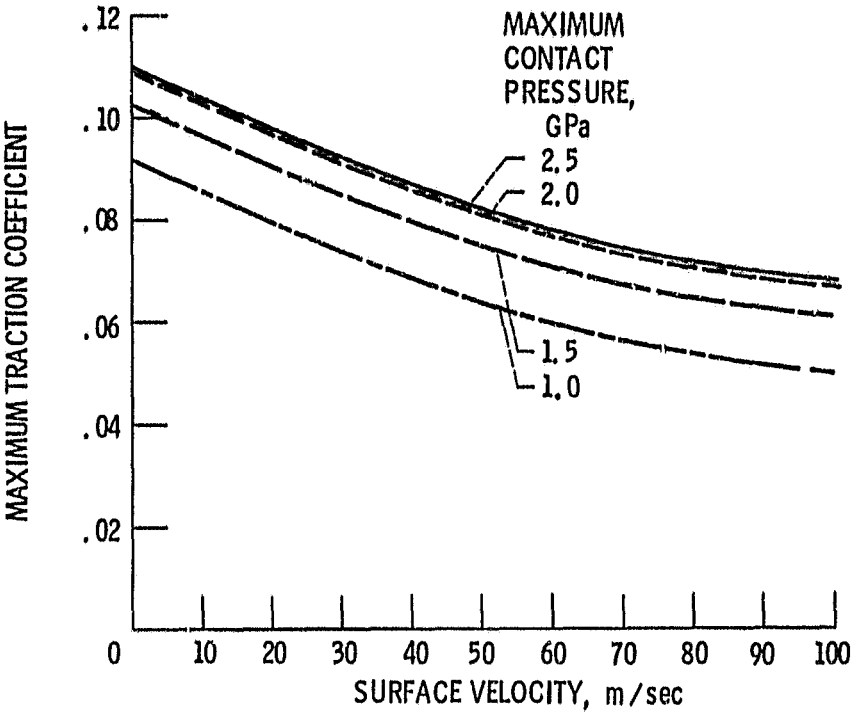

Figure 3. - Effect of surface velocity on maximum traction coefficient predicted from Santotrac 50 correlation. Temperature, 80 °C; ellipticity ratio, 5; spin, 0.

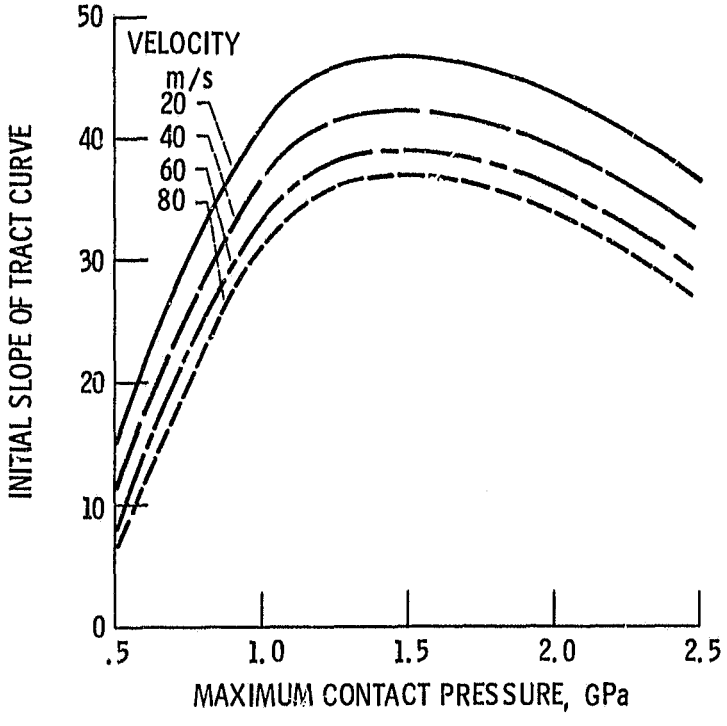

Figure 4. - Effect of pressure and velocity on slope from Santotrac 50 correlation. Temperature, 80 °C; ellipticity ratio, 5; spin, 0.

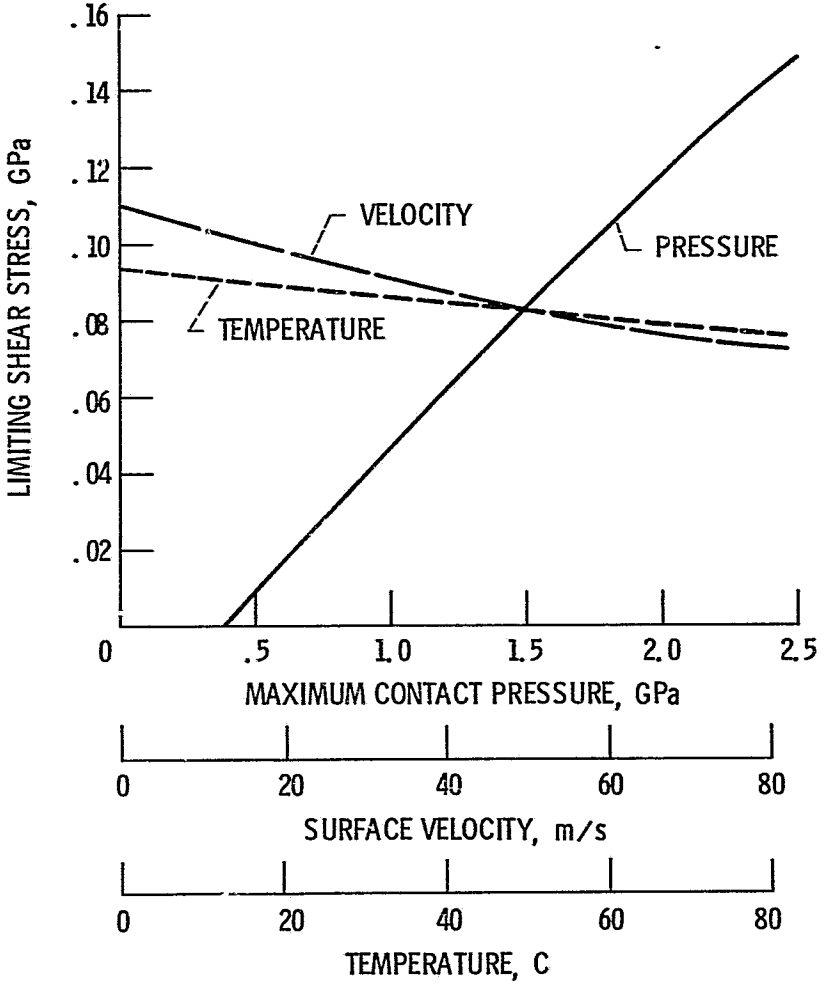

Figure 5. - Variation in limiting shear stress of Santorac 50. Pressure, 1.5 GPa; temperature, 50° C; velocity, 50 m/sec.

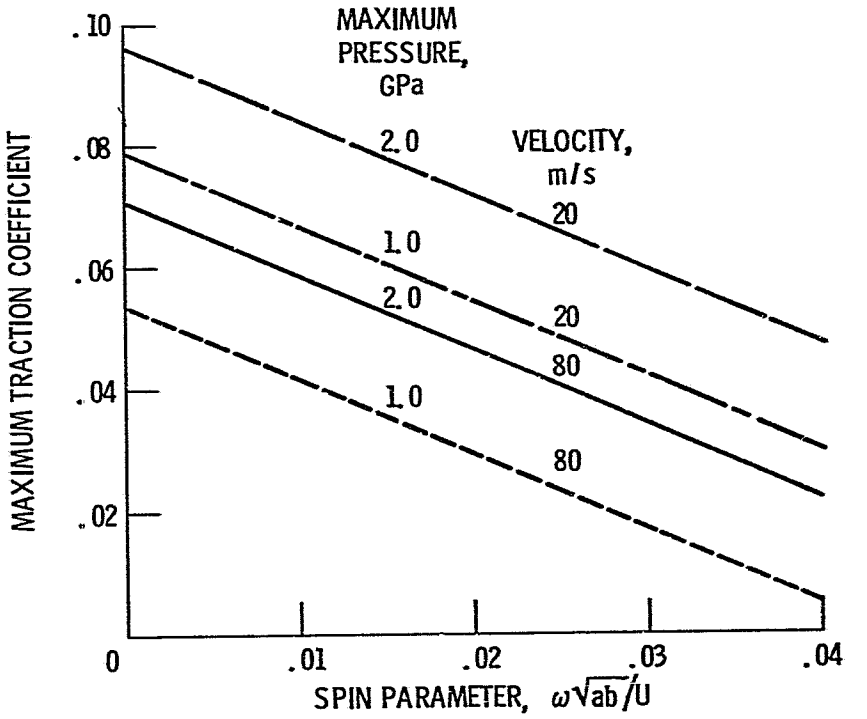

Figure 6. - Effect of spin on maximum traction coefficient from Santotrac 50 correlation. Temperature, 80 °C; ellipticity ratio, 5.

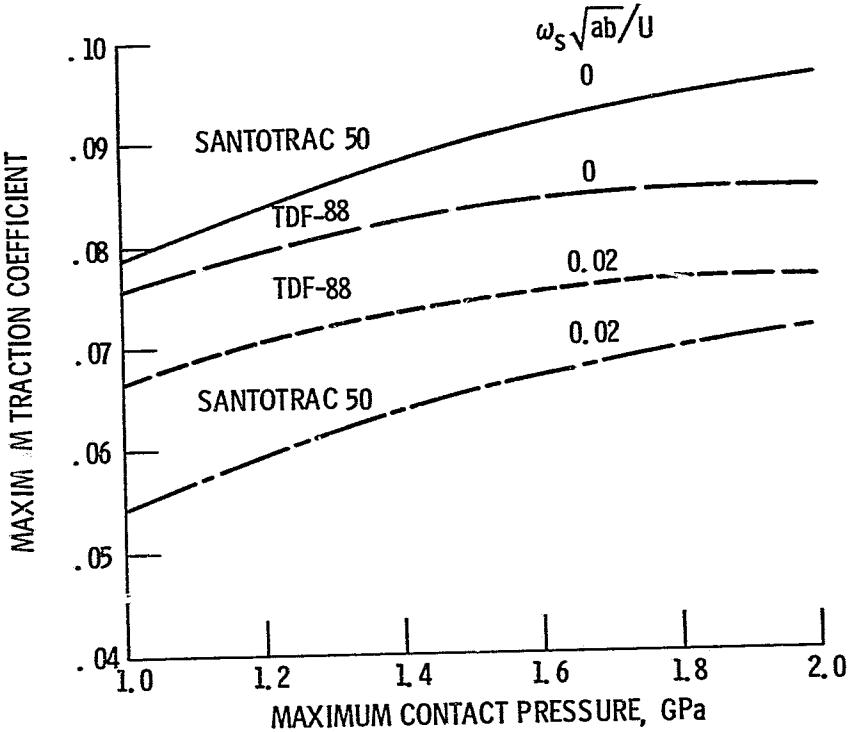

Figure 7. - Effect of spin on maximum traction coefficient for Santotrac 50 and TDF-88 fluids. Temperature, 80° C; velocity, 20 m/sec; ellipticity ratio, 5.

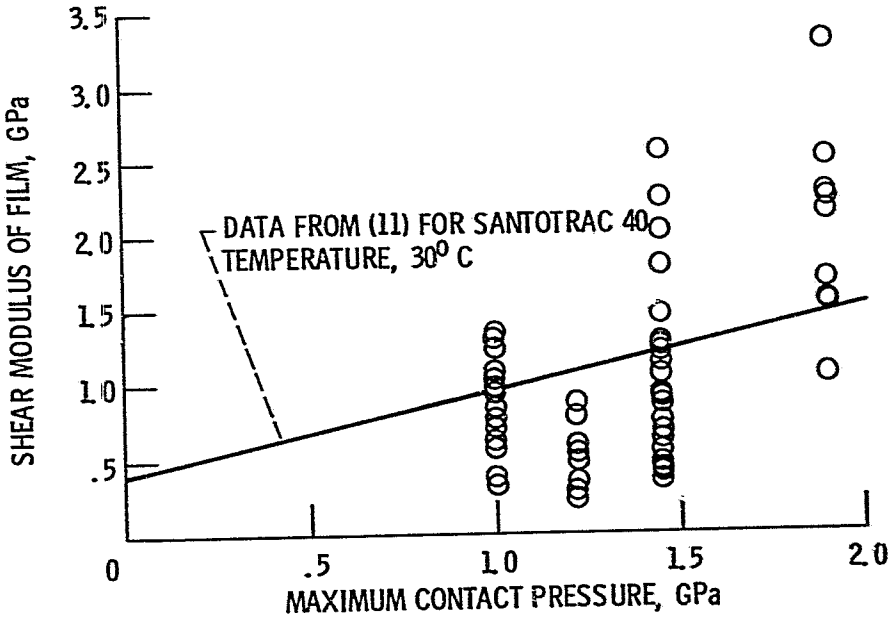

Figure 8. - Deduced shear modulus of film for Santotrac 50. Data from (18).

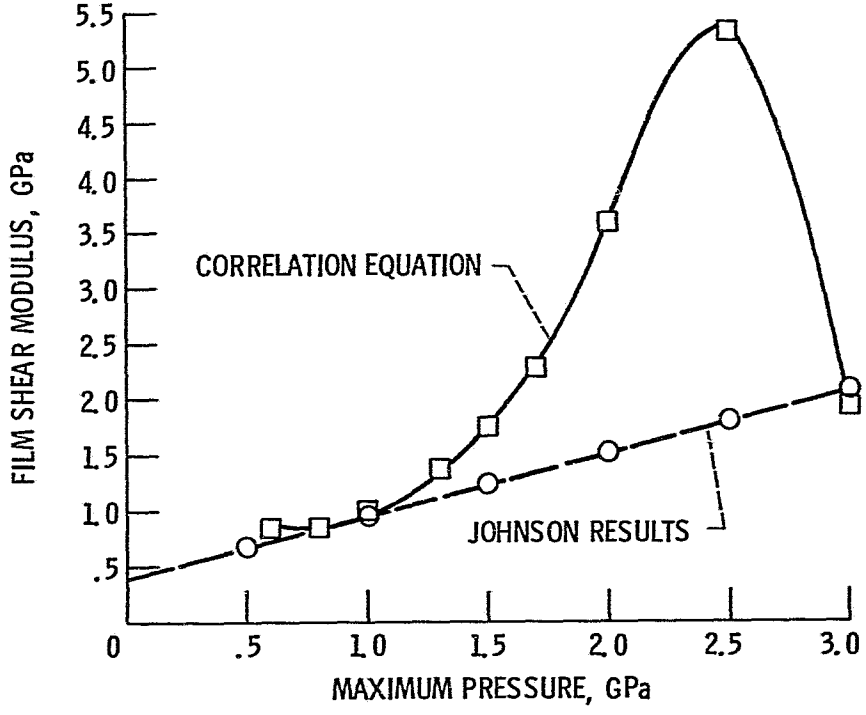

Figure 9. - Comparison of film modulus from correlation of Tevaarwerk data (Santotrac 50) with Johnson film modulus results (Santotrac 40). Temperature, 30° C; velocity, 20 m/sec; ellipticity ratio, 1. Data from (11).

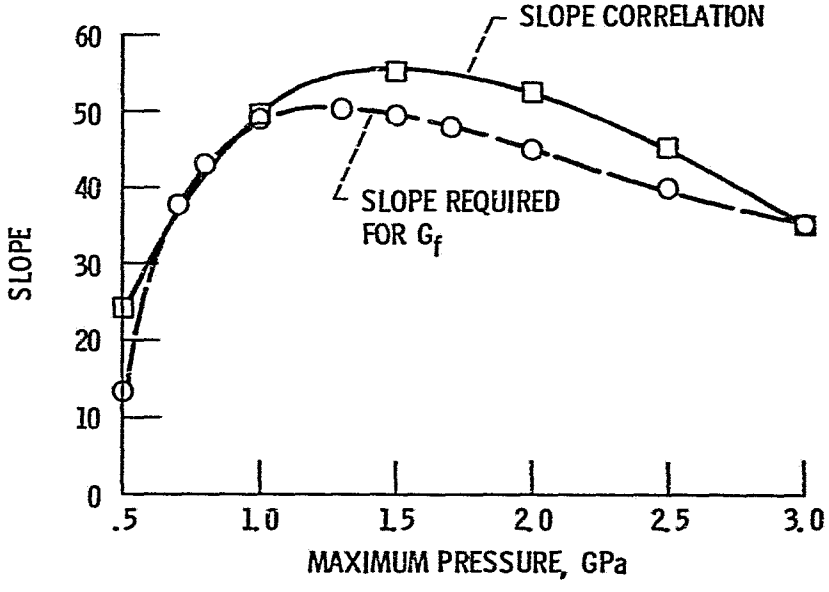

Figure 10. - Comparison of slope predicted from correlation of Tevaarwerk data (Santotrac 50) with slope required to produce Johnson film modulus results (11). Temperature, 30° C; velocity, 20 m/sec; ellipticity ratio, 1. Data from (11).